

# Hierarchically Biomimetic Bone Scaffold Materials: Nano-HA/Collagen/PLA Composite

S. S. Liao, F. Z. Cui, W. Zhang, Q. L. Feng

Biomaterials Laboratory, Department of Material Science & Engineering, Tsinghua University, Beijing 100084, People's Republic of China

Received 28 June 2002; revised 27 August 2003; accepted 4 September 2003

Published online 27 February 2004 in Wiley InterScience (www.interscience.wiley.com). DOI: 10.1002/jbm.b.20035

**Abstract:** A bone scaffold material (nano-HA/ collagen/PLA composite) was developed by biomimetic synthesis. It shows some features of natural bone both in main composition and hierarchical microstructure. Nano-hydroxyapatite and collagen assembled into mineralized fibril. The three-dimensional porous scaffold materials mimic the microstructure of cancellous bone. Cell culture and animal model tests showed that the composite material is bioactive. The osteoblasts were separated from the neonatal rat calvaria. Osteoblasts adhered, spread, and proliferated throughout the pores of the scaffold material within a week. A 15-mm segmental defect model in the radius of the rabbit was used to evaluate the bone-remodeling ability of the composite. Combined with 0.5 mg rhBMP-2, the material block was implanted into the defect. The segmental defect was integrated 12 weeks after surgery, and the implanted composite was partially substituted by new bone tissue. This scaffold composite has promise for the clinical repair of large bony defects according to the principles of bone tissue engineering. © 2004 Wiley Periodicals, Inc. *J Biomed Mater Res Part B: Appl Biomater* 69B: 158–165, 2004

**Keywords:** biomimetic; tissue engineering; nanocomposite; biodegradable; cell culture

## INTRODUCTION

Large bone fracture defects or bone tumor resections are serious problems for bone surgery, though autografts and allografts have long been widely used for bone reconstructive surgery.<sup>1</sup> The main drawback of autografts is donor shortage. For allograft, the problem is the potential risk of transmitting diseases and immunological response. Many bone-grafting materials, such as titanium alloy, ceramics, and polymers, have been used as bone-substitute materials.<sup>2</sup> However, each has a specific disadvantage. Permanent implantations can still erode *in vivo*, due to late breakdown and abscess formation. The acidic outcome of polymer biodegradation also negatively affected the latter-stage results of bone repair. It became necessary to find a promising alternative to the use of autogenous bone for grafting indications. Bone tissue engineering is a promising method for the repair of large bone defects.<sup>3,4</sup> Recently, studies of three-dimensional scaffold materials became a crucial element of bone tissue engineering

research. The three-dimensional scaffold materials were designed to mimic one or more of the bone-forming components of autograft, in order to facilitate the growth of vasculature into the material, and provide an ideal environment for bone formation.<sup>5–7</sup> Many researchers have prepared hydroxyapatite (HA) and collagen composite by mixture or self-organization, followed by cross linkage or uniaxial pressing to develop a large size material.<sup>8,9</sup>

Previous work has led to the development of a bone-like nano-hydroxyapatite/collagen (nHAC) composite by mineralizing the type I collagen sheet.<sup>10,11</sup> Preliminary *in vitro* and *in vivo* studies indicate that this material is bioactive and biodegradable. However, its mechanical properties were too weak for practical application. In order to improve the mechanical strength and the forming ability of the material, a new bone tissue engineering scaffold material, nano-HA/collagen/poly(lactic acid) (nHAC/PLA), has been developed. Its similarity to natural bone in main composition and hierarchical microstructure, its biomimetic preparation, and the biological testing of this material are reported in this article.

Natural bone is a complex biomineralized system with an intricate hierarchical structure. It is assembled through the orderly deposition of apatite minerals within a type I collagenous matrix. Bone mineral is a nonstoichiometric carbonated apatite with low crystallinity and nanometer size. The crystallographic *c* axis of the apatite is oriented to the axis of the collagen fibril.<sup>12,13</sup> In this novel material, the collagen molecules and nano-hydroxyapatite assembled into mineral-

This work was presented at the GRIBOI 12th Interdisciplinary Research Conference on Biomaterials held in Shanghai, China, March 14–17, 2002.

Correspondence to: Fuzhai Z. Cui, Biomaterials Laboratory, Department of Material Science & Engineering, Tsinghua University, Beijing 100084, People's Republic of China (e-mail: cuifz@mails.tsinghua.edu.cn)

Contract grant sponsor: National High-Technology Foundation of China; contract grant number: 2001AA320605

Contract grant sponsor: National Natural Science Foundation of China; contract grant number: NNSFC 20031010

© 2004 Wiley Periodicals, Inc.

ized fibril. Following that, the mineralized collagen fibril bundle was assembled in a parallel arrangement. Moreover, on the histological level, natural bone has an interconnecting porous structure also found in the top hierarchical level of the nHAC/PLA scaffold composite. PLA polymer is a biodegradable biomedical material used as a biodegradable suture in GTR (guided tissue regeneration) membranes and in fixation in orthopedics. High mechanical strength ensures the practical application of PLA in surgery.<sup>14,15</sup> This composite, combined with high compatibility and high strength, provided a promising scaffold in both traditional bone-defect repair and in bone tissue engineering.

## MATERIALS AND METHODS

### Synthesis

Synthesis of nHAC powder has been reported previously.<sup>10,11,16</sup> Type I collagen solution (CELLON Company) was adjusted to a concentration of 0.67 g collagen/l. Solutions of  $\text{CaCl}_2$  and  $\text{H}_3\text{PO}_4$  ( $\text{Ca/P}=1.66$ ) were then added separately by drops. The solution was gently stirred and titrated at room temperature with sodium hydroxide solution to pH 7.4. After 48 h, the nHAC deposition was harvested by centrifugation and freeze-dried. nHAC/PLA was made by the following procedure: PLA (ShangDong Medical Research Institute, China) of molecular weight 100,000 Da was dissolved in dioxane to final concentrations of 8%, 10%, and 12% (m/v). The solution was then stirred gently at room temperature for 4–6 h, and the nHAC powder was added at a 1:1 nHAC:PLA weight ratio. The solution was then ultrasonicated, poured into a mold, frozen at a temperature between 0 and  $-20^\circ\text{C}$  overnight, and then lyophilized to remove dioxane.

### Characterization

The porosity of nHAC/PLA was determined via a liquid displacement method with isopropyl alcohol (isopropanol,  $\rho = 0.784\text{ g/ml}$ ). A sample with a known weight  $w_1$  was immersed in a beaker holding a known volume of water  $v_1$ . A series of brief evacuation–repressurization cycles were performed to force the liquid into the pores of the composite. Then the total volume of the water plus the liquid-impregnated scaffold ( $v_2$ ) and the residual liquid volume after the water-impregnated composite was removed ( $v_3$ ) were recorded. The porosity of the composite ( $\epsilon$ ) is expressed as  $\epsilon = (v_1 - v_3)/(v_2 - v_3) \times 100\%$ .

The compressive mechanical property as tested with an Instron 1122 mechanical testing with a 10-kN load cell according to the guidelines set in ASTM D5024-95a. The specimens were cylinders about 9 mm in diameter and about 15 mm in length. The cross-head speed was set at 0.5 mm/min, and the load was applied until the foam was compressed to approximately 30% of its original length. The compressive modulus was calculated as the slope of the initial linear portion of the stress–strain curve. The compressive strength

was determined as the maximum point of the stress–strain curve.

Scanning electron microscopic (SEM) examinations (LEO 1530, Germany) were performed after coating the samples with gold. X-ray diffraction (XRD) patterns of the materials were recorded in a Rigaku D/max-RB diffractometer (Rigaku, Tokyo) with the use of Cu K radiation. Samples for transmission electron microscope (TEM) were also fixed with 2.5% glutaraldehyde in 0.1-M PBS (pH 7.0), followed by 1% osmium tetroxide in acetone. The specimens were dehydrated through a graded series of ethanol, embedded in Spon 812 (Serva, Feinbiochemical, Heidelberg, Germany). Ultra-thin sections were examined in a JEM-200CX TEM (JEOL, Japan). Selected-area electron diffraction (SAED) patterns were used to investigate the crystal orientation in the material.

### Cell Culture

Osteoblasts were isolated via sequential digestions of neonatal rat calvaria according to established procedures,<sup>17,18</sup> characterized by alkaline phosphatase activity as well as by deposition of calcium phosphate salts by the von Kossa staining technique, which is an indication of osteoblast mineralization, and cultured in Dulbecco's modified eagle medium (DMEM) supplemented with 10% fetal bovine serum (FBS) under standard cell culture conditions (that is,  $37^\circ\text{C}$ , humidified, 5%  $\text{CO}_2$ ). Osteoblasts were used at subcultured numbers 2–4.

The composite was cut into a disc (thickness = 1–2 mm), then sterilized by  $\gamma$ -ray irradiation (2.5 Mrad). The osteoblasts were seeded into the composite in a 3.5-cm dish at a concentration of  $5 \times 10^4$  cells/ $\text{cm}^2$ . The cultures were maintained in a humidified atmosphere consisting of 95% air/5%  $\text{CO}_2$  (v/v) at  $37^\circ\text{C}$ , and the medium was changed twice a week, and routinely examined by a Olympus IX-50 phase contrast microscopy (Olympus, Japan).

Samples for SEM were fixed with 2.5% glutaraldehyde in 0.1-M PBS (pH 7.0), followed by 1% osmium tetroxide in acetone. The specimens were dehydrated through a graded series of ethanol and acetonitrile, vacuum-pumped acetonitrile dried and gold coated for examination in a LEO 1530 (Leo, Germany).

### Implantation

Twenty-four white New Zealand adult rabbits (2.5–3 kg) were included in this study. The composite was fabricated into a cuboid with  $15\text{ mm} \times 5\text{ mm} \times 5\text{ mm}$ ; then 0.5 mg recombinant human bone morphogenetic protein (rhBMP-2) (China East Pharmacy Inc., Genetics Institute) solution was adsorbed by vacuum pump, followed by sterilization by epoxy ethane.

The implantation was under general anesthesia by an injection of 3% sodium pentobarbital (0.3 mg/kg body weight) in the auricular vein. After being positioned prone, the rabbits were shaved, prepped with povidone-iodine and draped in sterile fashion. The 15-mm segmental defect upper 1/3 of the radius in the right forelimb was created with a roller bit. The

composite was implanted in the segmental defect and observed at 4, 8, 12, and 16 weeks ( $n = 6$ ).

All of the harvested tissues were radiographed with an x-ray apparatus and then fixed with 10% neutral formalin, defatted with chloroform, demineralized with 10% ethylenediamine tetra acetic acid, and embedded in paraffin wax. Sections (5  $\mu\text{m}$  in thickness) were cut, stained with hematoxylin and eosin (H & E), and examined under a light microscope. New bone was defined by the radiographic appearance of a calcified mass that on histologic examination correlated with hematopoietic marrow and bony trabeculae.<sup>19</sup>

### Statistical Methods

ANOVA was used to compare to the results, with a significance level set to 5%. Repeated-measure STATA was employed to analyze the data for each of the character parameters.

## RESULTS

### Characterization

Figure 1 is an example of SEM morphology of nHAC/PLA (8%). It is seen from this figure that the composite is porous, with pore size of about 100–300  $\mu\text{m}$  [Figure 1(a)]. The pores are interconnected. The wall thickness of the pores is about 15–30  $\mu\text{m}$  [Figure 1(a,b)].

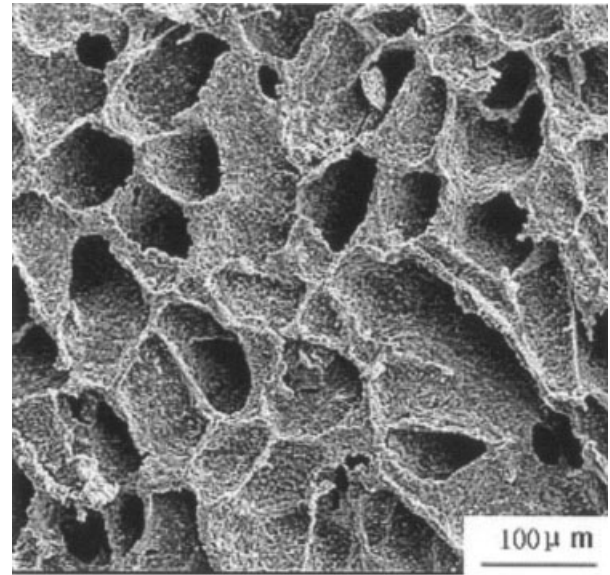
Under TEM, Figure 2(a) indicated the microstructure of the composite. The clusters of mineralized collagen fibrils were dispersed in the PLA matrix. The central part of Figure 2(a) is enlarged in Figure 2(c); the cluster consists of nearly parallel straight fibrils. The diameter of the fibrils is about 6 nm. The SAED indicated that the mineral crystals were [002]-oriented nano-HA crystals along the long axis of the collagen fibril [Figure 2(b)].

Phase development of the composite was demonstrated by XRD patterns (Figure 3). Compared to the HA crystal, the broadening of the diffraction peaks of nHAC implied a small grain size and low crystallinity. The pattern of the nHAC/PLA presents the same broadening peaks, which is also like the pattern of the natural bone. In natural bone, the nano-HA crystals and collagen make the overlap of the four peaks range from 32 to 35°.

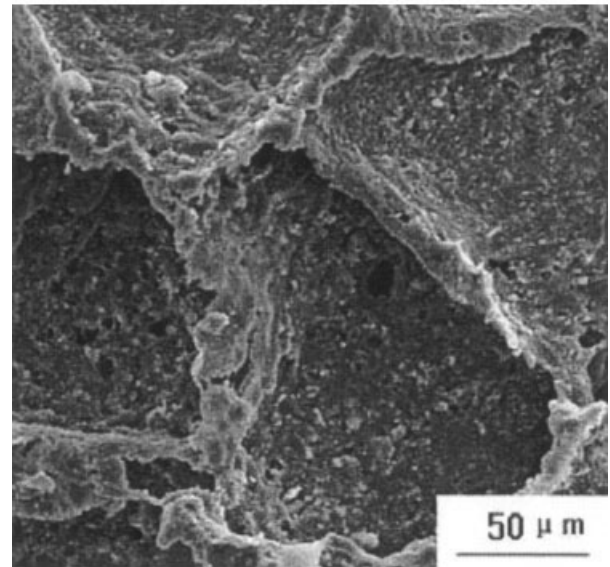
The mechanical properties of the composites of the three types (8%, 10%, 12% PLA in dioxane solvent) are different, as shown in Figure 4. The compressive strengths of the three types of composite increased with the increasing of PLA concentration. The elastic modulus values of these materials show a somewhat different trend of the compressive strength versus PLA concentration, 10% type sample was at the maximum value: 47.3 MPa. The porosity of these three types (8%, 10%, and 12% PLA) nHAC/PLA were all at 80% ( $\pm 2\%$ , all  $n = 3$ ).

### Cell Culture

Osteoblast growth in material-free organ culture can be distinguished into four stages.<sup>17–19</sup> Cells adhered to the flask



(a)



(b)

**Figure 1.** SEM morphology of the composite (a) nHAC/PLA scaffold; (b) enlargement of the central area of (a).

bottom or to the cell culture cover slip in a round shape during the initial 2 days. Then the round cell attached, spread, and proliferated on the bottom of the flasks or cover slips, exhibiting morphologies ranging from spindle shaped to polygonal. In 3 weeks, cells reached confluence. Polygonal cells packed closely into a mosaic appearance. At 4 weeks, the extracellular matrix was fibrous between the multilayer cells.

SEM indicated the cells experienced similar development in the co-culture system of cell and composite. Two days after seeding, cells adhered on the surface of the composite. The cells proliferated in the following days and grew into the inner pores of the scaffold. After 1 week, the cells reached

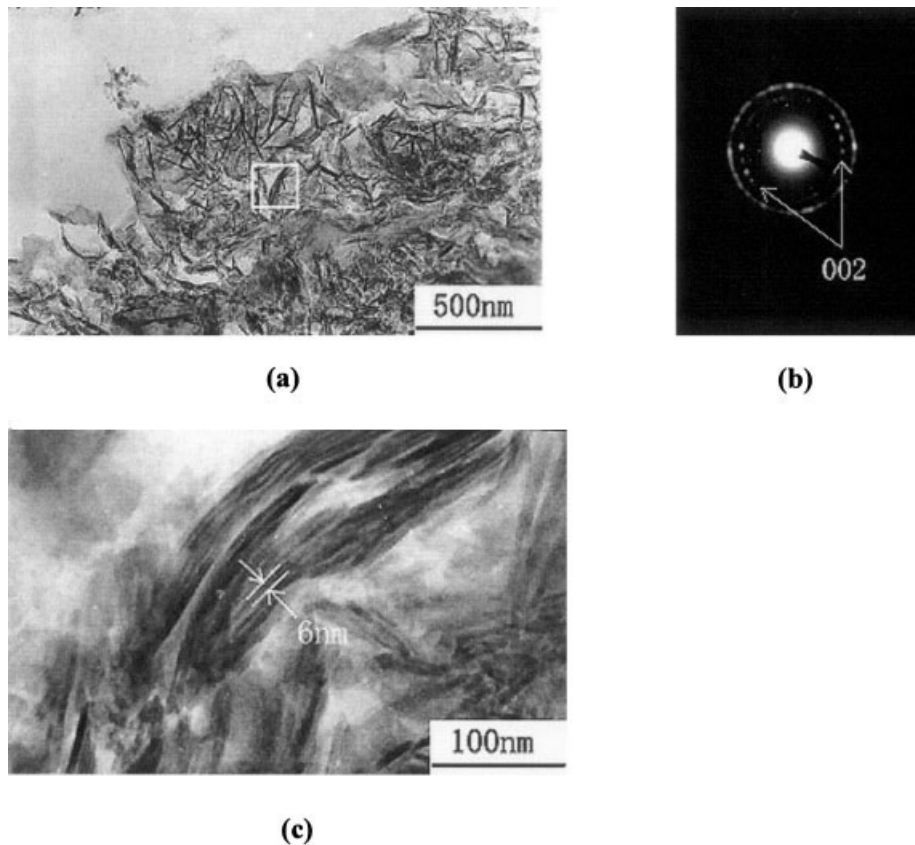


**Figure 2.** TEM micrographs of nHAC/PLA composite: (a) and (c) an ultra-thin section of Epon-embedded composite; (b) SAED pattern of the central part of (a).

confluence on the material [Figure 5(b), black arrow], while the material-free group did not reach this status [Figure 5(a)]. The cells adhered to the membrane with processes and multiple filopodia [Figure 5(c)], and anchored onto the pore wall [Figure 5(d), white arrows]. The fibrillar bundles of extracellular matrix were attached to the material and connected to each other.

#### *In Vivo* Analysis

The X-ray and histological observations demonstrated that the 15-mm segmental defect was completely healed within 12

weeks after surgery [Figure 6(b, d)]. Compared to the X-ray graph of the defect just after surgery [Figure 6(a)], the X-ray graph 12 weeks after implantation shows the double cortical bone connected [Figure 6(b)]. The porous composite was partially replaced by new bone tissue. At 8 weeks, a large number of round cells had grown into the pores of the material, and adhered to the walls of the pores [Figure 6(c)]. The cells congregated at the interface between the composite and the new bone tissue. Corresponding to the decrease of material, the bone marrow and trabeculae fill up the location. Comparison of the histology of the 8 and 12-week samples [Figure 6(e)] shows that there is more implanting material replaced by new trabeculae.

#### DISCUSSION

Traditional bone-defect repair procedures utilize autogenous bone as a graft to provide the osteoinductive and osteoconductive components necessary for the formation of new bone at the operative site; it has long been the gold standard for orthopedics. Complications associated with the harvest of autograft, such as limited quantities, donor-site morbidity, blood loss, and increased operative time, have prompted the search for the suitable alternatives. New bone graft materials are being designed to mimic one or more of the bone-forming components of autograft.

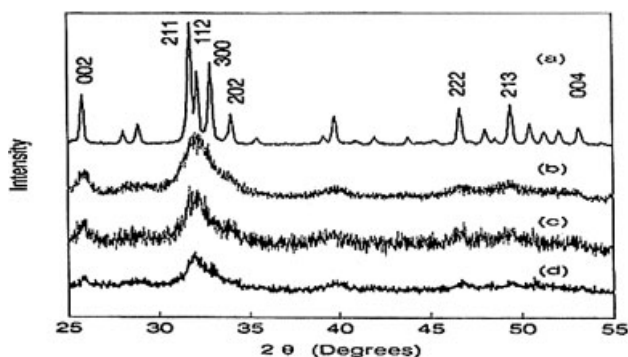


**Figure 3.** XRD graph of (a) commercial HA, (b) nHAC, (c) nHAC/PLA, and (d) natural bone.

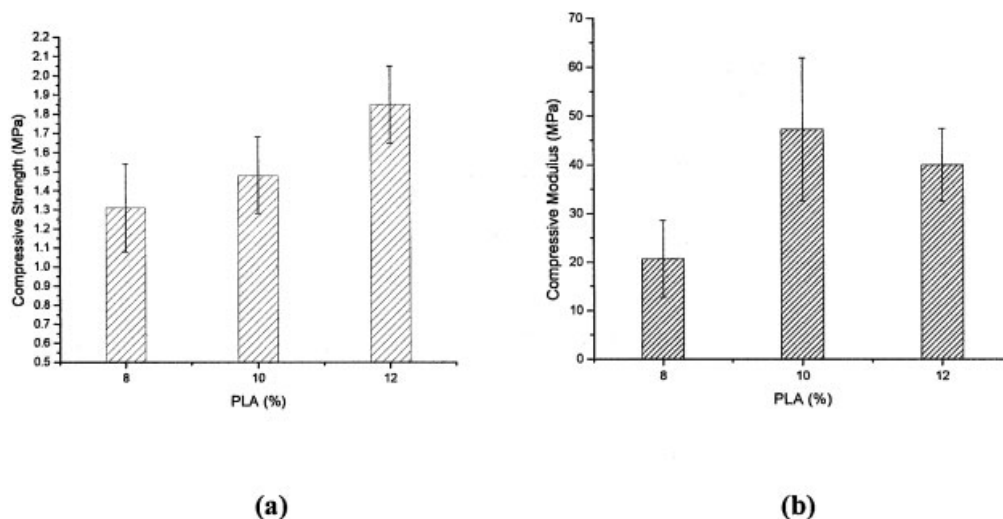


**Figure 4.** The compressive property testing results of the materials. (a) The compressive strength value of nHAC/8%, 10%, and 12% PLA; (b) the elastic modulus of nHAC/8%, 10%, and 12% PLA.

The results, show that the nHAC/PLA and the natural bone are similar in main composition and in hierarchical microstructure. Type I collagen is the major structural protein of bone tissue, making up about 30% of the dry weight of bone and 90–95% of its nonmineral content.<sup>12</sup> In the nHAC/PLA composite, the main component is the type I collagen and

hydroxyapatite. The poly lactic acid is only about 12% of the weight of the final block material. Figure 7 shows the nano-to microscale hierarchical microstructure of the scaffold material. First, the collagen molecules and nano-hydroxyapatite assembled into mineralized fibrils, that were about 6 nm in diameter and about 300 nm long. The collagen molecules in

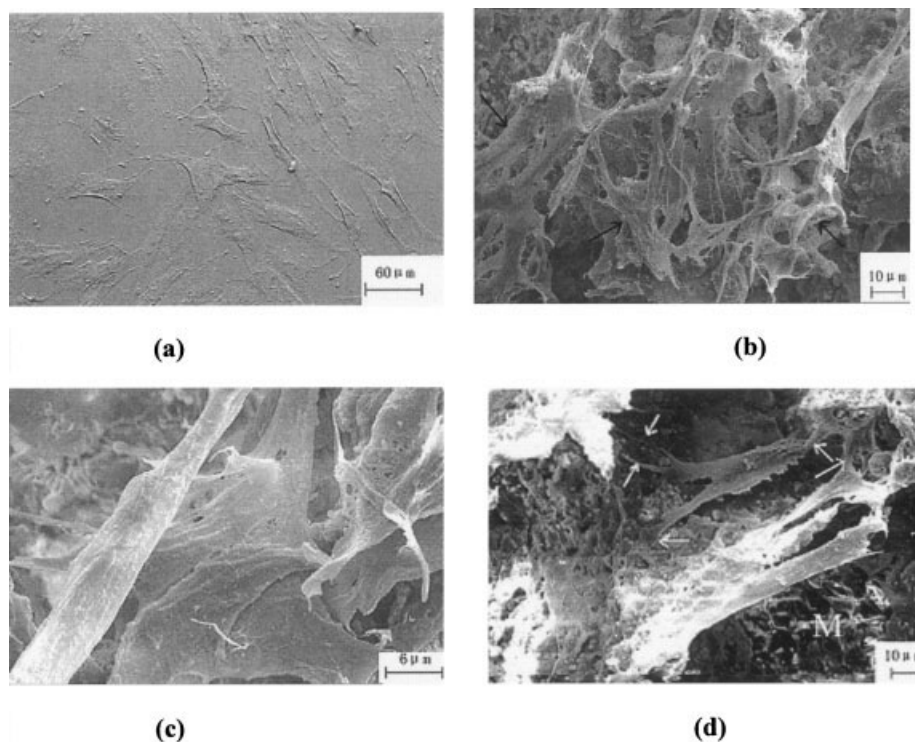


**Figure 5.** SEM results of a 1-week cell culture on the nHAC/PLA composite: (a) control group—osteoblasts on glass; (b) osteoblasts on nHAC/PLA surface; (c) magnification of (b); (d) osteoblasts adhered to the pores of the nHCA/PLA composite. Black arrows indicate cell proliferation. White arrows indicate the oriented fibrillar bundles of extracellular matrix that are attached to the material and connected with the cell.

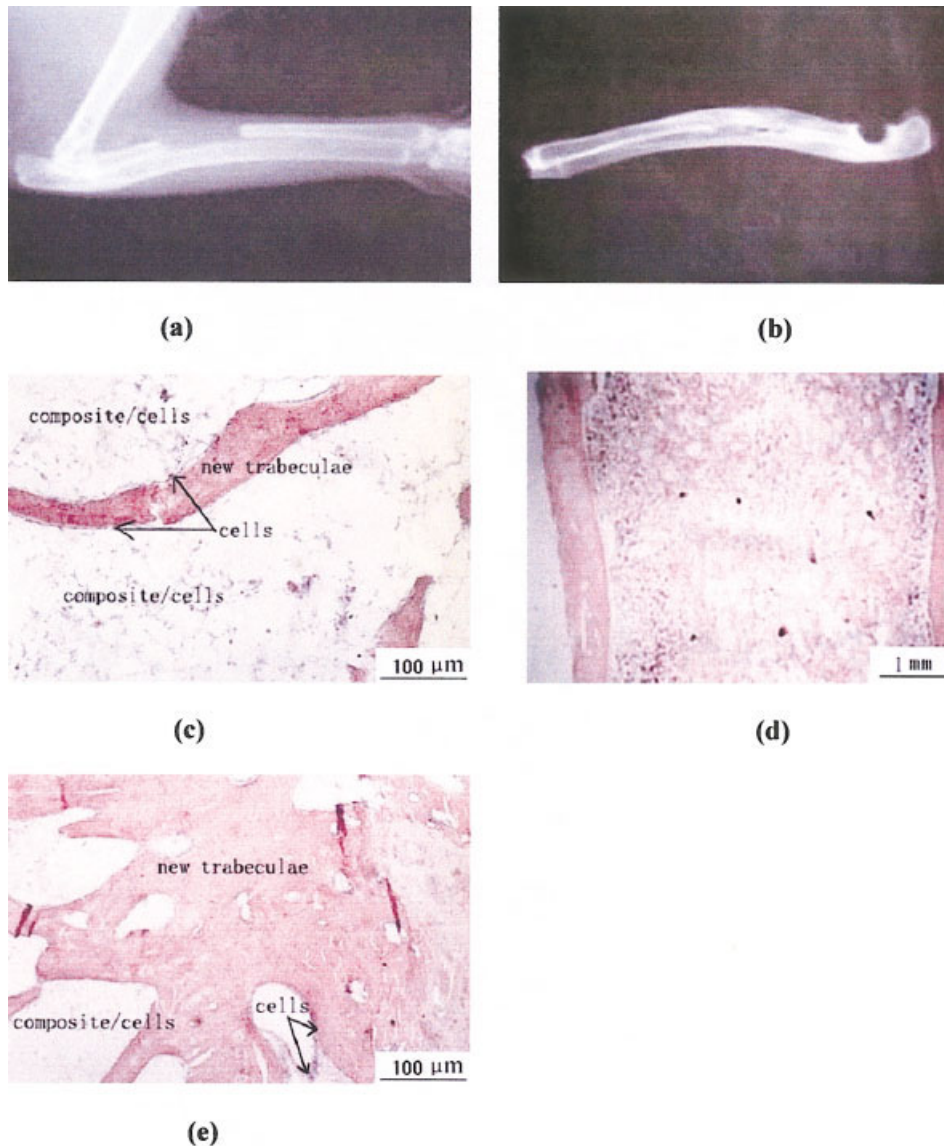


**Figure 6.** Results of the nHAC/PLA composite experiments: (a) after surgery; (b) implant at 12 weeks, double cortical bone connected completely; (c) implant at 8 weeks, decalcified histology HE staining; (d) implant at 12 weeks, histology HE staining, double cortical bone connected completely, bone marrow and new bone trabeculae in vertex zone; (e) implant at 12 weeks, decalcified histology HE staining (compare to 8 weeks, more new trabeculae replace the composite).

bone were secreted by the cell, and were, like the fibrils, of nanometer size. Second, the mineralized collagen fibril parallel was assembled into fibril bundles, along a straight line. The fibril array patterns also show the same pattern in bone. The assembled mineralized collagen fibrils uniformly distribute in the PLA matrix. The average pore size of scaffold is above 100 μm. The high porosity of the scaffold is a result of an interconnected three-dimensional pore structure. This porous scaffold is similar to that of spongy bone—the highest level of the bone hierarchy. A suitable macroporous structure is important in order to obtain good implant incorporation through rapid vascularization, bone ingrowth, and, where the implant is resorbable, possible remodeling.<sup>5–7</sup>

Based on the basic biomineralization principles, an nHAC composite had previously been developed by mineralizing

type I collagen sheets. Preliminary studies indicate that this nHAC material is bioactive and biodegradable. However, its mechanical property was too weak for practical application, especially on compressive strength. An ideal material for bone tissue engineering should be nonimmunogenic, biodegradable, highly effective in osteoinduction with relatively low dose of inducing signals, ready for vascular and mesenchymal cell invasion, carvable, and amenable to contouring for optimal adaptation to various shapes of bone defects, providing mechanical support when needed.<sup>20,21</sup> A new bone tissue engineering scaffold material, nHAC/PLA, has been developed. The nHAC/PLA composite fulfills most of the requirements for use as a suitable substratum for bone tissue engineering. The first advantage of this composite is the high biocompatibility. nHAC possesses a high effective affinity



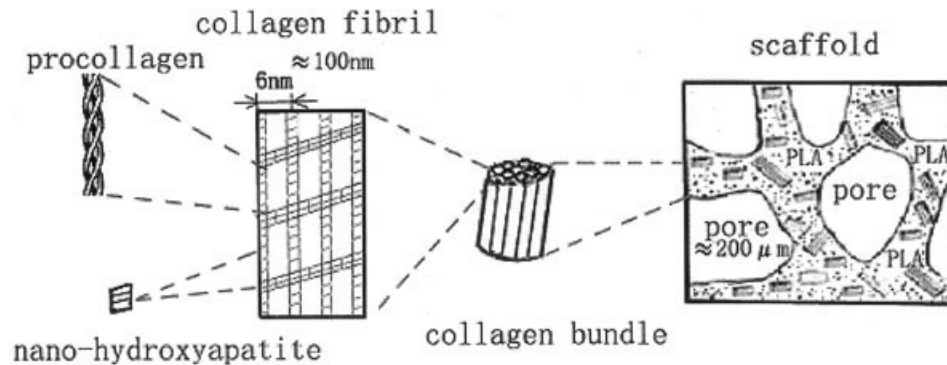


Figure 7. Hierarchical structure of the nHAC/PLA composite.

for regulating cell function and promoting osteogenesis. Kikuchi and Mehlish have implanted a mixture of HA particles and collagen and reported high biocompatibility.<sup>8,22</sup> Design of biomaterials with surface properties similar to physiological bone (characterized by surface grain sizes in the nanometer regime<sup>23</sup>) would undoubtedly aid in the formation of new bone at the tissue/biomaterial interface and, therefore, improve orthopedic/dental-implant efficacy. In the present preparation, the freeze-drying technique keeps the nHAC component as initial status on the final composite, and the three-dimensional scaffold was made by the simple and applied method. Different ratios of PLA dissolved in the solution result in different compressive strengths, so this polymer has far-ranging clinical applications. This is another advantage of this composite for bone tissue engineering. If the clinical application requires a stronger or weaker composite, a higher or lower molecular weight of PLA, PLGA, or other biocompatible polymer can be used to attain different mechanical strengths and biodegradability ratios. The compressive strength of the nHAC/PLA composite reached the lower limit of natural cancellous bone (1 MPa).<sup>24</sup> The compressive modulus of trabecular bone is approximately 50 MPa,<sup>25</sup> which is comparable to that of the present nHAC/PLA (10%) composite.

The osteoblast performed the normal stages of adhesion, proliferation, and maturation that accompanied the morphological change from mainly spindle shaped to predominantly polygonal on the nHAC/PLA scaffold material. In culture media, the surface of composite gradually appeared more smooth by biodegradation (data not shown). The cells were spread out in the interconnected pores. In the process of co-culture, the outcome of biodegradation apparently did not change the pH value of the media, which is one of the essential factors ensuring normal growth. This composite indeed overcame the disadvantage of the acid outcome degradation seen with the use of pure PLA devices. The acidic degraded PLA might be neutralized by the presence of the nano-mineralized collagen in the composite. Of course, more experiments are necessary to examine this question.

In the implant experiment, the large segmental defects (length = 15 mm, critical size) of rabbits healed quickly after 12 weeks. It is demonstrated that the composite is an

appropriate bone substitute material for ingrowth of new bone. The porous surface of the implant material could provide a suitable environment for collagen and bone mineral deposition, as well as osteoblast attachment. The cells also could modulate further development of bone tissue.<sup>26–29</sup> As the osteoclast-like cells reabsorb the bone matrix, and the osteoblasts are associated with bone formation. The interconnected pores also provide tunnels to carry the nutrients and cells. After the cells enter into the composite, the nanometer-sized HA with low crystallinity has more affinity for bone mineral formation with collagen, which differs from bioceramics with well-crystallized and coarse grains (in the  $\mu\text{m}$  range).<sup>30</sup> A composite less mineralized than natural bone could promote degradation in tissue. Signaled by a low concentration of BMP, the new bone produced by osteoblasts effect on this composite as soon as possible.<sup>31</sup> Schimandle et al.<sup>32</sup> reported that fusions achieved using rhBMP-2 delivered in the collagen carrier were more remodeled and homogeneous compared with using rhBMP-2 delivered in autograft with or without a collagen carrier, and fusions achieved with rhBMP-2 were biomechanically stronger and stiffer than fusions achieved using autogenous bone graft. Sandhu et al.<sup>33</sup> reported on the efficacy of rhBMP-2 with an open-cell PLA in a canine posterolateral spinal fusion model. Following the principles of bone tissue engineering, use of a compound of composite, cells, and signal molecules is promising for the cure of defects larger than those that can be helped by traditional methods. Although bone morphogenic proteins were first purified and identified by Urist in 1965,<sup>34</sup> the rhBMP-2 used here has only recently been clinically used.

In this article, preliminary research on the novel nHAC/PLA composite was described. In the near future, other mechanical properties of this material will be investigated, including bending testing. The quantitative data on degradation and ossification *in vivo* must also be measured. Moreover, as these materials are bioactive and biodegradable materials, the dose of BMP other growth factor combined with the material should be an important aspect of the research.

## CONCLUSIONS

A new type of nano-composite bone material, nHAC/PLA was fabricated with the use of a biomimetic strategy. The nano-composite shows some features of natural bone both in main composition and hierarchy microstructure. The porous microstructure of this material is similar to that of cancellous bone. The cell culture and the implant experiments demonstrated that the composite was bioactive. The composite scaffold is a promising material for bone tissue engineering.

The assistance of Dr. X. D. Zhu (cell culture), and C. Zhang (implant surgery) is gratefully acknowledged.

## REFERENCES

1. Damien JC, Parson JR. Bone graft and bone graft substitutes: A review of current technology and application. *J Appl Biomater* 1991;2:187–208.
2. Hench LL, Wilson J. Surface-active biomaterials. *Science* 1984; 226:630–636.
3. Stock UA, Vacanti JP. Tissue engineering: Current state and prospects. *Annu Rev Med* 2001;52:443–451.
4. Langer R, Vacanti JP. Tissue engineering. *Science* 1993;260: 920–926.
5. Grenga T, Zins JE, Bauer TW. The rate of vascularisation of coralline hydroxyapatite. *Plast Reconstr Surg* 1989;84:245–249.
6. Schliephake H, Neukam FW, Klosa D. Influence of pore dimensions on bone ingrowth into porous hydroxyapatite blocks used as bone substitutes. A histometric study. *Int J Oral Maxillofac Surg* 1991;20:53–58.
7. Tancred DC, McCormack BAO, Carr AJ. A synthetic bone implant macroscopically identical to cancellous bone. *Biomater* 1998;19:2303–2311.
8. Kikuchi M, Itoh S, Ichinose S, Shinomiya K, Tanaka J. Self-organization mechanism in a bone-like hydroxyapatite/collagen nanocomposite synthesized in vitro and its biological reaction in vivo. *Biomater* 2001;22:1705–1711.
9. Chang MC, Ikoma T, Kikuchi M, Tanaka J. Preparation of a porous hydroxyapatite/collagen nanocomposite using glutaraldehyde as a crosslinkage agent. *J Mater Sci Lett* 2001;20:1199–1201.
10. Du C, Cui FZ, Zhu XD, de Groot K. Three-dimensional nano-HAp/ collagen matrix loading with osteogenic cells in organ culture. *J Biomed Mater Res* 1999;44:407–415.
11. Du C, Cui FZ, Zhang W, Feng QL, Zhu XD, de Groot K. Formation of calcium phosphate/collagen composites through mineralization of collagen matrix. *J Biomed Mater Res* 2000; 50:518–527.
12. Landis WJ, Song MJ, Leith A. Mineral and organic matrix interaction in normally calcifying tendon visualized in three dimensions by high-voltage electron microscopic tomography and graphic image reconstruction. *J Struct Biol* 1993;110:39–54.
13. Lowenstam HA, Weiner S. On biomineralization. New York: Oxford University Press; 1989. p 35–40.
14. Fini M, Giannini S, Gioradano R, Giavaresi G, Grimaldi M, Nicoli AN, Orienti L, Rocca M. Resorbable device for fracture fixation: *In vivo* degradation and mechanical behaviour. *Int J Artif Organs* 1995;18:772–776.
15. Taddei P, Monti P, Simoni R. Vibrational and thermal study on the *in vitro* and *in vivo* degradation of a poly (lactic acid)-based bioabsorbable periodontal membrane. *J Mater Sci Mater Med* 2002;13:469–475.
16. Zhang W, Liao SS, Cui FZ. Hierarchical self-assembly of nano-fibrils in mineralized collagen Chem Mater, to be published.
17. Ishaug SL, Yaszemski MJ, Bizios R, Mikos AG. Osteoblast function on synthetic biodegradable polymers. *J Biomed Mater Res* 1994;28:1445–1453.
18. Puleo DA, Holleran LA, Doremus RH, Bizios R. Osteoblast responses to orthopaedic implant materials in vitro. *J Biomed Mater Res* 1991;25:711–723.
19. Naoto S, Takao O, Hiroshi H. A biodegradable polymer as a cytokine delivery system for inducing bone formation. *Nature Biotech* 2001;19:332–335.
20. Vacanti CA. The impact of biomaterials research on tissue engineering. *MRS Bull* 2001;26:798–799.
21. Ripamonti U, Duneas N. Tissue engineering of bone by osteo-inductive biomaterials. *MRS Bull* 1996;21:36–39.
22. Mehlish DR, Leider AS, Roberts WE. Histologic evaluation of the bone/graft interface after mandibular augmentation with hydroxylapatite/purified collagen implants. *Oral Surg Oral Med Oral Pathol* 1990;70:685–692.
23. Webster TJ, Siegel RW, Bizios R. Osteoblast adhesion on nanophase ceramics. *Biomater* 1999;20:1221–1227.
24. Gibson J. The mechanical behaviour of cancellous bone. *J Biomech* 1985;18:317–328.
25. Shea LD, Wang D, Franceschi RT, Mooney DJ. Engineering bone development from a pre-osteoblast cell line on three-dimensional scaffolds. *Tissue Eng* 2000;6:605–617.
26. Jones SJ, Boyde A. The migration of osteoblasts. *Cell Tissue Res* 1977;184:197–182.
27. Ishaug SL, Crane GM, Miller MJ. Bone formation by three-dimensional stromal osteoblast culture in biodegradable polymer scaffolds. *J Biomed Mater Res* 1997;37:17–28.
28. Kwong CH, Burns WB, Cheung HS. Solubilization of hydroxyapatite crystals by murine bone cells, macrophages and fibroblasts. *Biomater* 1989;10:579–584.
29. Du C, Su XW, Cui FZ, Zhu XD. Morphological behaviour of osteoblasts on diamond-like carbon coating and amorphous C-N film in organ culture. *Biomater* 1998;19:651–658.
30. Cui FZ, Du C, Su XW, Zhu XD, Zhao NM. Biodegradation of a nano-hydroxyapatite/collagen by peritoneal monocyte-macrophages. *Cell Mater* 1996;6:31–44.
31. Reddi AH. Morphogenesis and tissue engineering of bone and cartilage: inductive signals, stem cells, and biomimetic biomaterials. *Tissue Eng* 2000;6:351–359.
32. Schimandle JH, Boden SD, Hutton WC. Experimental spinal fusion with recombinant human bone morphogenetic protein-2. *Spine* 1995;20:1326–1337.
33. Sandhu HS, Linda EA, Kanim MA. Evaluation of rhBMP-2 with an OPLA carrier in a canine posterolateral (transverse process) spinal fusion model. *Spine* 1995;20:2669–2682.
34. Urist MR. Bone formation by autoinduction. *Science* 1965;150: 893–899.